LETTER TO THE EDITOR

Intensive induction therapy with FLAG-idarubicin-venetoclax for fit older high-risk patients with acute myeloid leukemia

Authors

Avraham Frisch,[1] Baher Krayem,[1,2] Tsila Zuckerman,[1,3] Israel Henig,[1] Dana Yehudai-Ofir[1,3] and Netta Glaubach[1]

[1]Department of Hematology and Bone Marrow Transplantation, Rambam Health Care Campus, Haifa, Israel; [2]Division of Hematologic Malignancies, Memorial Sloan Kettering Cancer Center, New York, NY, USA and [3]The Ruth and Bruce Rappaport Faculty of Medicine, Technion, Israel Institute of Technology, Haifa, Israel

Correspondence:
A. FRISCH - a_frisch@rambam.health.gov.il

https://doi.org/10.3324/haematol.2025.300442

Received: December 25, 2025.
Accepted: February 23, 2026.
Early view: March 5, 2026.

Aberrant fucosylation of extracellular vesicles remodels the vascular microenvironment and promotes chemoresistance in myelodysplastic syndromes and acute myeloid leukemia

Jingjing Feng[1,2#], Kexin Wang[1#], Junjie Gou[1,3#], Yi Wang[4], Bowen Hu[1], Wei Wei[1], Junqi Ge[1], Yanli Feng[4], Shuang Feng[1], Eric Solary[2], Feng Guan[1], Xiang Li[1,5*]

1. Key Laboratory of Resource Biology and Biotechnology of Western China, Ministry of Education; Provincial Key Laboratory of Biotechnology, College of Life Sciences, Northwest University, Xi'an, China.
2. INSERM U1287, Université Paris-Saclay, Gustave Roussy Cancer Center, Villejuif, France.
3. Xi'an No. 1 Hospital, First Affiliated Hospital of Northwest University, School of Medicine, Xi'an, China.
4. Department of Hematology, Provincial People's Hospital, Xi'an, China.
5. Institute of Hematology, School of Medicine, Northwest University, Xi'an, China.

The authors have declared that no conflict of interest exists.

# Authors contributed equally.

*Correspondence to Xiang Li (e-mail: xiangli@nwu.edu.cn), Tel: +86-29-88303534, College of Life Science, Northwest University, 229 Taibai North Road, Xi'an, Shaanxi 710069, China

Supplemental methods

Cell lines and cell culture

Human leukemia-derived cell line KG1a and DAC-resistant KG1a (KG1a-DAC)[1] were cultured in RPMI 1640 medium, human umbilical vein endothelial cell line HUVEC and embryonic kidney cell line HEK-293T were cultured in DMEM (Biological Industries; Kibbutz Beit Haemek, Israel). All medium was supplemented with 10% fetal bovine serum (FBS) (Biological Industries). All cells were maintained at 37°C in a 5% CO_2 atmosphere and routinely tested for Mycoplasma with the GMyc-PCR Mycoplasma Test Kit (#40601ES20, Yeasen, Shanghai, China).

Preparation of conditioned medium (CM) and sEVs

Cells were incubated in FBS-free medium for 48 h. The supernatant was collected and centrifuged at 500 × g for 10 min, and then filtered with 0.22 μm filter as CM.

To prepare sEVs, CM was sequentially centrifuged at 2000 × g for 20 min, 10,000×*g* for 30 min at 4 °C, and ultracentrifuged twice at 100,000 × g (Optima XE-100; Beckman Coulter Life Sciences; Indianapolis, IN, USA) for 70 min.[2] Pellets were resuspended in PBS and stored at -80 °C.

Characterization of sEVs

Isolated sEVs were placed on 400-mesh carbon-coated grids (Electron Microscopy Sciences; Fort Washington, PA, USA) and stained with 2% uranyl acetate. Images were captured using a transmission electron microscopy (TEM) (model H-7650; Hitachi; Tokyo). Nanoparticle tracking analysis (NTA) was performed using the Zetaview-PMX120-Z instrument (Particle Metrix, Meerbusch, Germany).

Permeability assay

HUVECs (6×10^4) were plated on 0.4 μm transwell filters in a 12-well plate (Jet Biofil), and treated with CM or sEVs (50 μg/mL) for 48 h. Rhodamine B (RB)-dextran (70 kDa; Sigma-Aldrich, St. Louis, MO, USA) was added to the upper well to a final concentration of 10 μg/mL. Following an incubation period of 30 minutes, the fluorescence intensity in the lower chamber was quantified using a microplate reader, with an excitation wavelength at 544 nm and an emission wavelength at 590 nm.

Transendothelial migration analysis

HUVECs (3×10^4) were plated on 8 μm transwell filters in a 12-well plate (Jet Biofil) to form a monolayer, and treated with CM or sEVs (50 μg/mL) for 48 h. Subsequently, 1×10^4 stable GFP-expressing KG1a cells were added into upper chamber and cultured for 24 h. Afterward, the cells migrated to the lower chamber were harvested, and the GFP fluorescence intensity of these cells was assessed using flow cytometry.

Tube formation assay

HUVECs were incubated with serum-free medium for 12 h, and then seeded at 2×10^4 cells per well in 96-well plates precoated with Matrigel matrix (Corning, NY, USA). These cells were treated with CM or sEVs (50 μg/mL) for 4–6 h. Tube formation was observed and documented photographically under a microscope.

SDS-PAGE and Western blotting

Cells were collected and lysed with RIPA buffer (50 mM Tris, pH 7.2, 1% Triton X-100, 0.5% sodium deoxycholate, 0.1% SDS, 150 mM NaCl, 10 mM $MgCl_2$ and 5% glycerol) containing 1% PMSF. Protein concentration was determined using BCA

Protein Assay Kit (#P0011, Beyotime, Nanjing, China). Proteins (25 μg) from each lysate were separated by electrophoresis in a 10% polyacrylamide resolving gel and transferred onto a polyvinylidene difluoride (PVDF) membranes. After blocking with 3% BSA (#ST023, Beyotime) in Tris-buffered saline containing 0.1% Tween-20 (TBST) at RT for 1 h, membranes were incubated at 4°C overnight in TBS-T containing following antibodies against Alix (#92880S, Cell Signaling Technology, MA, USA), Calnexin (#2679S), IκBα (#9242), p65 (#8242), p- IκBα (#2859), p- p65 (#3031), FUT4 (#19497-1-AP, proteintech, Wuhan, China), CD15 (#sc-19595), Occludin (#sc-133256), Claudin-5 (#sc-374221), ZO1 (#sc-33725, Santa Cruz Biotechnology, USA), TSG101 (#T55985, Abmart, Shanghai, China), followed by the addition of secondary antibody conjugated with HRP (#A0208, #A0216, Beyotime). Bands were visualized by enhanced chemiluminescence (ECL; Vazyme Biotech, Nanjing, China).

Detection of Le^X on sEVs by lectin-based ELISA

To determine the levels of Le^X on sEVs, 96-well ELISA plates were pre-coated with 100 μL/well of anti-CD63 antibody (sc-365604, Santa Cruz Biotechnology) and incubated for 12 h at 4 °C. The plates were washed three times with PBST (0.05% Tween-20 in PBS) and blocked with 1% BSA for 1 h at 37 °C. sEVs samples were added and incubated for 2 h at 37 °C. After washing with PBST, the wells were incubated with biotinylated Aleuria aurantia lectin for 2 h at 37 °C, followed by incubation with HRP-conjugated streptavidin for 30 min at 37 °C. The plates were developed using 3,3′,5,5′-tetramethylbenzidine (TMB) substrate (Promega, Madison, USA) and the reaction was stopped with 2 M H_2SO_4. Absorbance was measured at

450 nm using a microplate reader.

Proteomic analysis

Proteins (100 µg) were denatured with 8 M urea, reduced by 5 mM dithiothreitol (DTT) for 1 h at RT, alkylated with 20 mM iodoacetamide (IAM) for 30 min in the dark at RT, diluted with deionized water to lower urea concentration below 2 M, digested with lysyl endopeptidase (Wako Puro Chemical; Osaka, Japan) for 4 h at 37 °C, and digested with trypsin (Promega) overnight at 37 °C. The mixture was acidified with 10% trifluoroacetic acid (TFA) to pH< 3 and purified using C18 cartridges (Waters Corp.; Taunton, MA, USA). Two-dimensional liquid chromatography/ mass spectrometry (LC-MS) was performed on LTQ8 Orbitrap MS (Thermo Fisher; San Jose, CA, USA) and data were analyzed using Proteome Discoverer software (Thermo Fisher), with quantification by MaxQuant software program v2.6.7.0 (maxquant.org).[3]

N-glycan analysis

Glycomic analysis was performed as previously described.[4] A volume of 10 µL serum or 1 mg of sEVs was added onto a size-exclusion spin ultrafiltration unit (Millipore; Billerica, MA, USA). Proteins were denatured with 8 M urea/ 50 mM NH4HCO3, reduced with dithiothreitol (DTT), alkylated with iodoacetamide (IAM), and digested with PNGase F overnight at 37 °C. Released N-glycans were collected by centrifugation, lyophilized, and desalted using HyperSep Hypercarb solid phase extraction (SPE) cartridge (ThermoFisher Scientific; Waltham, Massachusetts, US).

Lyophilized N-glycans were dissolved and spotted onto an MTP AnchorChip sample target with 20 mg/mL 2,5-dihydroxybenzoic acid (DHB) as the matrix.

Measurements were taken in positive-ion mode. Each full-mass scan was performed with following conditions: acceleration voltage, 24.59 kV; reflector voltage, 26.6 kV; pulsed ion extraction, 100 ns; mass range, 1000–3500 m/z. For the data analysis, the peaks were smoothed and baseline subtraction performed three times. Relative intensity was analyzed and generated using FlexAnalysis software (Bruker Daltonics; Bremen, Germany) based on MALDI-TOF/TOF–MS intensity. m/z data were annotated using GlycoWorkbench software,[5] and cross-referenced with previous studies. [6-8]

Chromatin immunoprecipitation assay (ChIP)

The ChIP assay was performed as described previously.[9] Briefly, KG1a-TWIST1 cells[10] were cross-linked with 1% formaldehyde. Subsequently, DNA was fragmented to an average length of 200 to 500 bp using a sonicator (#Ymnl-1000Y, Nanjing, China). Immunoprecipitation was performed using antibody against TWIST1 (#ab50887, Abcam). Protein A/G agarose was added and rotated for 4 h. The samples were subsequently treated with proteinase K (#ST532, Beyotime) and RNase A (#ST578, Beyotime). Target DNA was extracted using phenol/chloroform and analyzed by PCR with the primers in Tab. S2.

Dual luciferase reporter assay

The wild type and mutant regions of FUT4 promoter were amplified by PCR and cloned into pGL3 vector (#E1751, Promega; Madison, WI, USA). Then the pGL3 vector containing the wild-type or mutant FUT4 promoter regions was co-transfected into HEK-293T cells along with the Renilla luciferase expression plasmid (pRL-TK, #D2760, Beyotime) and the TWIST1 overexpression plasmid. After 48 h, luciferase activity was

measured with a Dual Luciferase Reporter Assay System (#RG028, Beyotime). The primers for PCR have been shown in Tab.S3.

OptiPrep density gradient purification

sEVs were purified by OptiPrep density gradient as described previously.[11] In brief, 40%, 20%, 10%, and 5% (w/v) iodixanol solutions were prepared by diluting OptiPrep (60% (w/v) aqueous iodixanol, Axis-Shield PoC; AS; Oslo, Norway) with 0.25 M sucrose/ 10 mM Tris, pH 7.5 in 14 × 89 mm Ultra-Clear tubes. sEVs purified by ultracentrifugation were placed on top of the gradient, continuous gradient was established through ultracentrifugation at 100,000 × g for 18 h using a Beckman Coulter Optima XE-100 and Ti45 rotor, and twelve fractions were collected. Each fraction was diluted in PBS, pelleted through another round of ultracentrifugation at 100,000 x g for 3 h, and washed with and resuspended in PBS.

Supplementary figures with legends.

Fig. S1. (A) Permeability of HUVEC monolayers to rhodamine B–labeled dextran (RB-dextran) after coculture with KG1a or KG1a-DAC for 48 h. (B) Immunoblot analysis of tight junction proteins in HUVECs cocultured with KG1a or KG1a-DAC. (C) Representative images of tube formation. (D) Immunoblot analysis of tight junction–related proteins in HUVECs treated with conditioned medium (CM) from KG1a or KG1a-DAC. (E) RB-dextran permeability and (F) transendothelial migration after CM treatment. (G) Quantification of junction count and total branching length in HUVECs treated with CM. Data are mean ± SEM; experiments were repeated three times with similar results. **P<0.01; ***P<0.001.

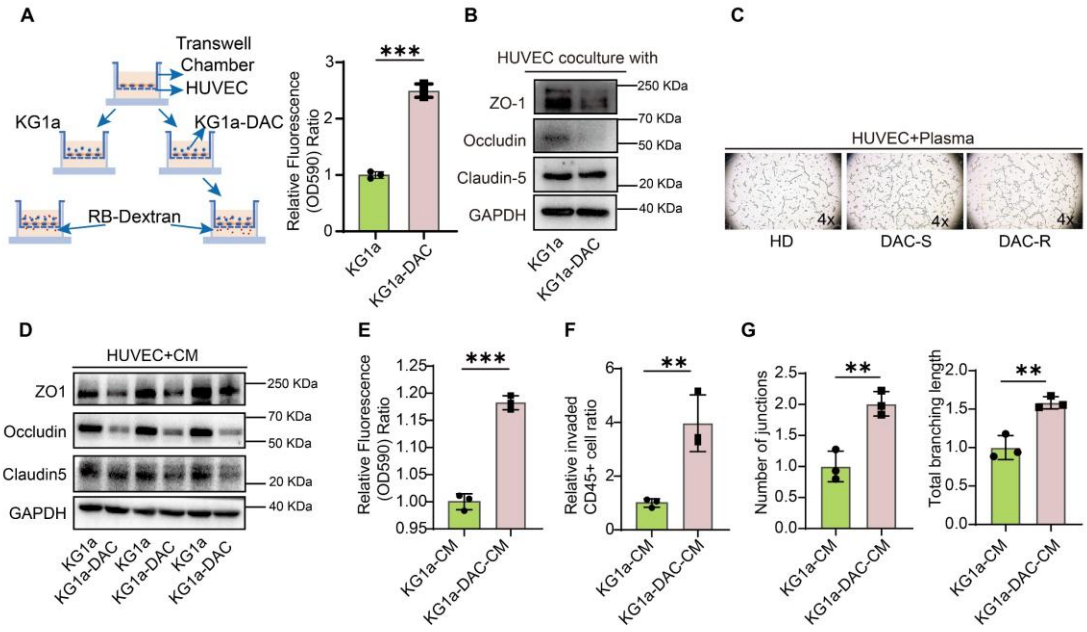

Fig. S2. (A-F) Characteristic of small extracellular vesicles (sEVs) using TEM (A&B), NTA (C&D), and western blotting (E&F). (G)Tube formation assay.

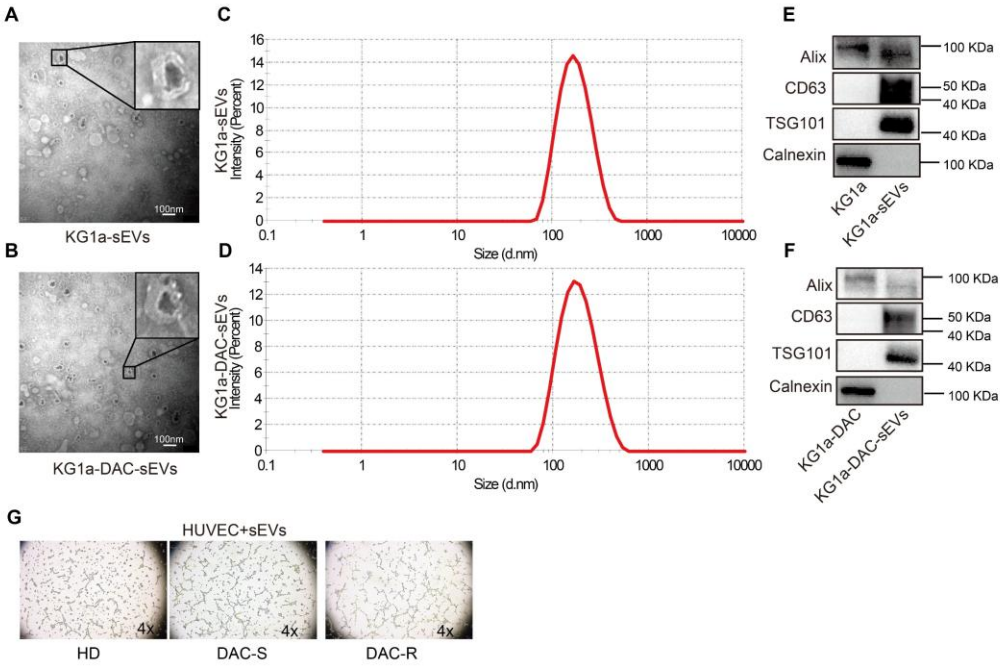

Fig. S3. (A-C) MALDI-TOF/TOF–MS spectra of N-glycans in myelodysplastic syndromes/acute myeloid leukemia (MDS/AML) patients who are sensitive to DAC treatment (DAC-S) or are refractory to DAC treatment (DAC-R) serum samples. Peaks

of MALDI-TOF/TOF–MS spectra (signal-to-noise ratio>5) were selected for relative intensity analysis. Glycan compositions are annotated using the H/N/F/S nomenclature (H, hexose; N, N-acetylglucosamine; F, fucose; S, sialic acid).

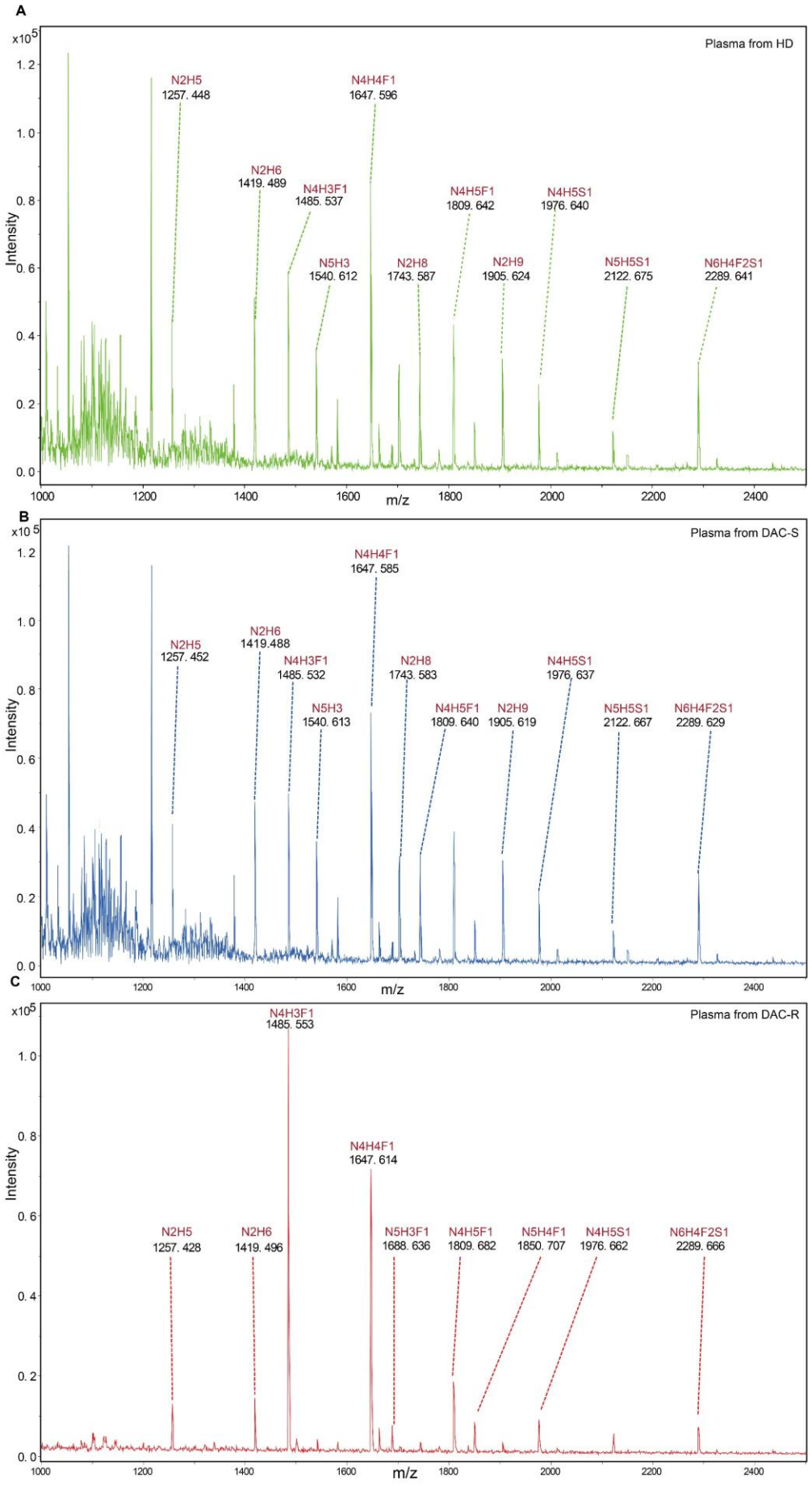
A
Plasma from HD
x10^5
Intensity
m/z
N2H5 1257. 448
N4H4F1 1647. 596
N2H6 1419. 489
N4H3F1 1485. 537
N4H5F1 1809. 642
N4H5S1 1976. 640
N5H3 1540. 612
N2H8 1743. 587
N2H9 1905. 624
N5H5S1 2122. 675
N6H4F2S1 2289. 641
B
Plasma from DAC-S
N4H4F1 1647. 585
N2H5 1257. 452
N2H6 1419.488
N4H3F1 1485. 532
N2H8 1743. 583
N4H5S1 1976. 637
N5H3 1540. 613
N4H5F1 1809. 640
N2H9 1905. 619
N5H5S1 2122. 667
N6H4F2S1 2289. 629
C
Plasma from DAC-R
N4H3F1 1485. 553
N4H4F1 1647. 614
N2H5 1257. 428
N2H6 1419. 496
N5H3F1 1688. 636
N4H5F1 1809. 682
N5H4F1 1850. 707
N4H5S1 1976. 662
N6H4F2S1 2289. 666

Fig. S4. (A) Relative abundance of fucosylated and non-fucosylated N-glycans in plasma from healthy donors (HD), decitabine-sensitive (DAC-S), and decitabine-refractory (DAC-R) patients. (B) Relative intensity of individual fucosylated N-glycan compositions in plasma from HD, DAC-S, and DAC-R patients. (C) Fold change of individual fucosylated N-glycan compositions normalized to the HD group. (D) Representative MALDI-TOF/TOF–MS spectra of N-glycans in sEVs from KG1a and KG1a-DAC cells. Peaks with signal-to-noise ratio >5 were included for relative intensity analysis. Glycan compositions are annotated using the H/N/F/S nomenclature (H, hexose; N, N-acetylglucosamine; F, fucose; S, sialic acid). (E) Relative intensity of individual N-glycan compositions in sEVs from KG1a and KG1a-DAC cells. (F) AAL-reactive signal in plasma from HD, DAC-S, and DAC-R samples determined by ELISA. (G) Immunoblot analysis of FUT4 expression in KG1a and KG1a-DAC cells. (H) Le^X levels in KG1a-DAC cells with or without PNGase F treatment. (I) Le^X levels in plasma-derived sEVs from HD, DAC-S, and DAC-R samples. (J) Le^X levels in KG1a and KG1a-DAC cells assessed by flow cytometry (representative histograms and mean fluorescence intensity quantification). Data are mean ± SEM; experiments were repeated three times with similar results. ns, not significant; *P<0.05; **P<0.01; ***P<0.001.

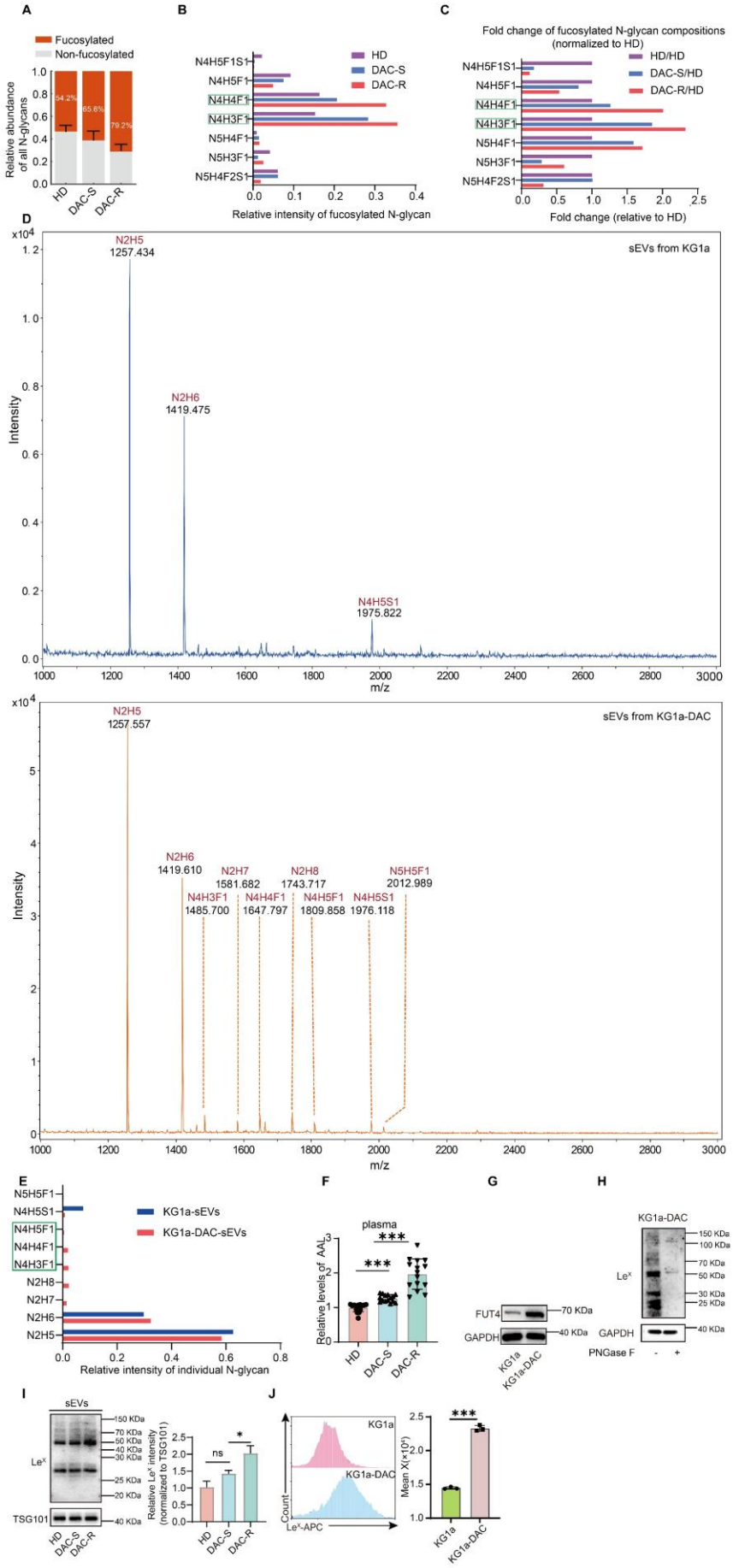
A
Fucosylated
Non-fucosylated
Relative abundance of all N-glycans
54.2%
65.6%
79.2%
HD
DAC-S
DAC-R
B
HD
DAC-S
DAC-R
N4H5F1S1
N4H5F1
N4H4F1
N4H3F1
N5H4F1
N5H3F1
N5H4F2S1
Relative intensity of fucosylated N-glycan
C
Fold change of fucosylated N-glycan compositions (normalized to HD)
HD/HD
DAC-S/HD
DAC-R/HD
Fold change (relative to HD)
D
sEVs from KG1a
N2H5
1257.434
N2H6
1419.475
N4H5S1
1975.822
Intensity
m/z
sEVs from KG1a-DAC
N2H5
1257.557
N2H6
1419.610
N2H7
1581.682
N2H8
1743.717
N5H5F1
2012.989
N4H3F1
1485.700
N4H4F1
1647.797
N4H5F1
1809.858
N4H5S1
1976.118
E
KG1a-sEVs
KG1a-DAC-sEVs
N5H5F1
N4H5S1
N4H5F1
N4H4F1
N4H3F1
N2H8
N2H7
N2H6
N2H5
Relative intensity of individual N-glycan
F
plasma
Relative levels of AAL
HD
DAC-S
DAC-R
G
FUT4
70 KDa
GAPDH
40 KDa
KG1a
KG1a-DAC
H
KG1a-DAC
Le^x
GAPDH
PNGase F
I
sEVs
Le^x
TSG101
HD
DAC-S
DAC-R
Relative Le^x intensity (normalized to TSG101)
ns
J
KG1a
KG1a-DAC
Count
Le^x-APC
Mean X(×10^4)

Fig. S5. (A) Immunoblot analysis of tight junction–related proteins in human umbilical vein endothelial cells (HUVECs) after exposure to conditioned medium (CM) from KG1a or KG1a-FUT4. (B, C) HUVEC permeability to rhodamine B–labeled dextran (OD590) and transendothelial migration (relative invaded $CD45^+$ cell ratio) after exposure to the indicated CM. (D) Angiogenesis metrics (junction count and total branching length) in HUVECs treated with the indicated CM. (E, F) FUT4 expression and Lewis X (Le^X) levels in KG1a-DAC-shFUT4 cells and their derived small extracellular vesicles (sEVs). (G, H) Immunoblot analysis of tight junction–related proteins in HUVECs after exposure to CM or sEVs from KG1a-DAC or KG1a-DAC-shFUT4. (I, J) HUVEC permeability (OD590) and transendothelial migration (relative invaded $CD45^+$ cell ratio) after exposure to the indicated sEVs or CM. (K, L) Angiogenesis metrics (junction count and total branching length) in HUVECs treated with the indicated CM or sEVs. (M) Immunoblot analysis of tight junction–related proteins in HUVECs treated with OptiPrep-purified sEVs from KG1a, KG1a-DAC, KG1a-FUT4, and KG1a-DAC-shFUT4 cells. (N) Quantification of human $CD45^+$ cells in blood, bone marrow, and spleen in mice preconditioned with HD-sEVs or KG1a-sEVs. Data are mean ± SEM; experiments were repeated three times with similar results. *P<0.05; **P<0.01; ***P<0.001.

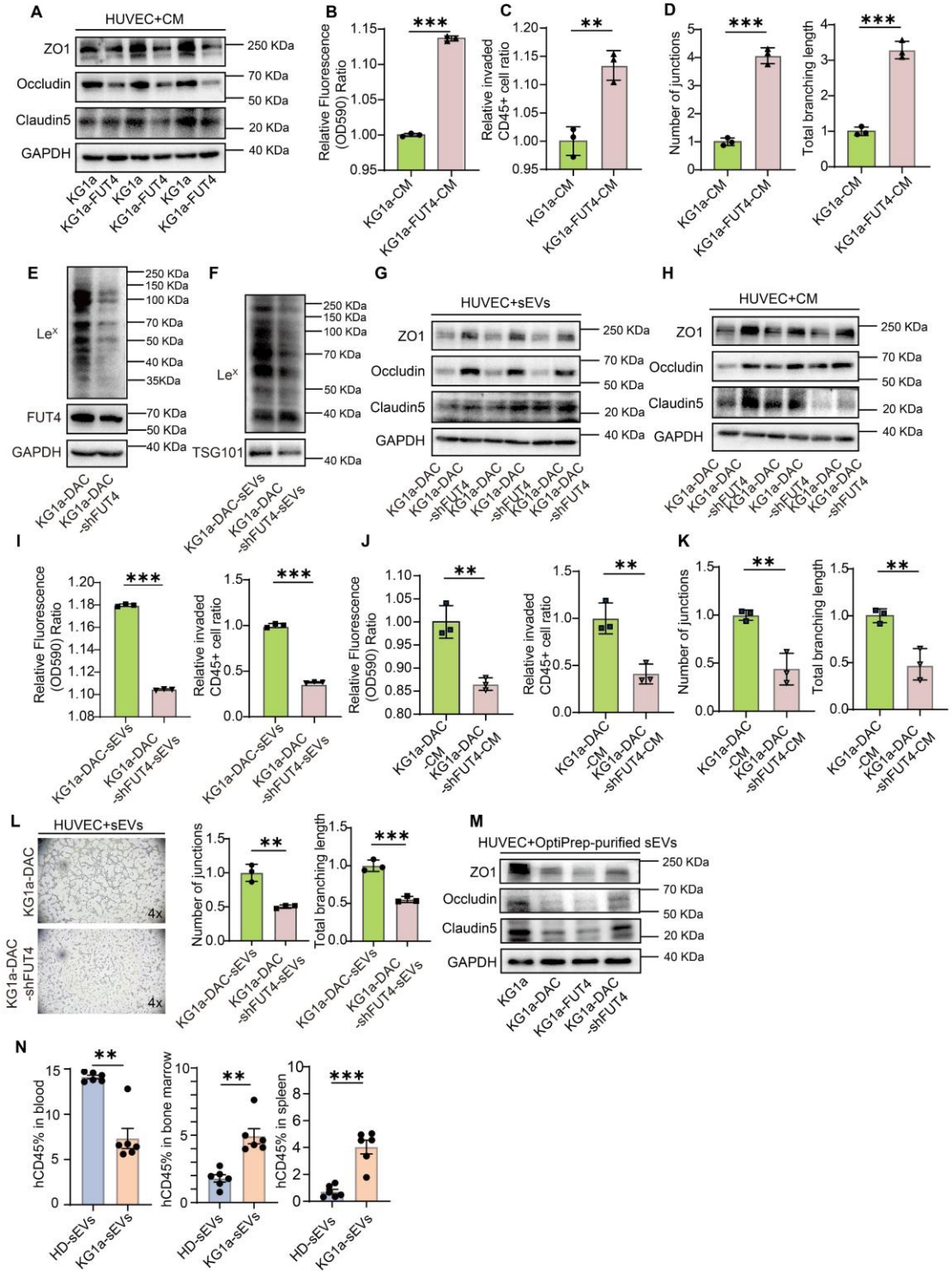

Fig. S6. (A) Expression of FUT4 and TWIST1 at mRNA levels in KG1a and KG1a-TWIST1 cells. (B&C) Expression of FUT4, TWIST1 at protein and mRNA levels and the levels of Le^X in SKM1 and SKM1-shTWIST1 cells. (D) Tight junction related-proteins and (E&F) permeability in HUVECs after treated with CM from SKM1 and

SKM1-shTWIST1. (G) Angiogenesis metrics in HUVECs treated with CM from SKM1 and SKM1-shTWIST1. (H) TWIST1 binding to E-box motifs within the 0–2000 bp region of the FUT4 promoter. (I) TWIST1 binding sites on wild-type (WT) and mutant sequences of E-box motif 1, 2 and 7 of FUT4 promoter. Data are mean ± SEM; experiments were repeated three times with similar results. *P<0.05; **P<0.01; ***P<0.001.

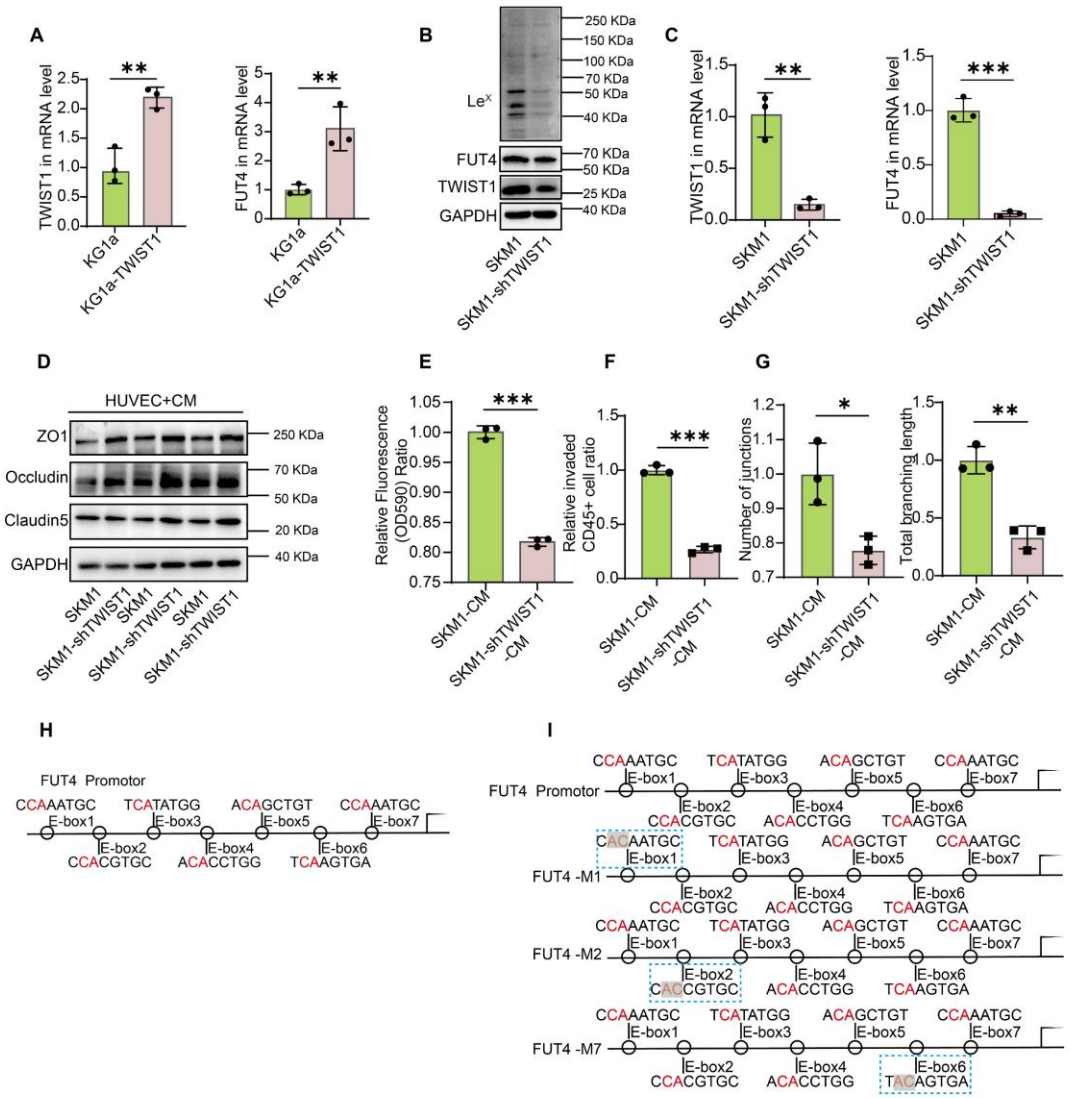

Fig. S7. (A) Immunoblot analysis of density gradient fractions showing sEV markers and ICAM3 in sEVs isolated from KG1a cells. (B) Expression of ICAM3 and Le^X in OptiPrep-purified sEVs derived from KG1a, KG1a-DAC, KG1a-FUT4, and KG1a-DAC-

shFUT4 cells. (C) Expression of ICAM3 in ultracentrifugation-isolated sEVs from the indicated cells. (D) ICAM3 stability in KG1a and KG1a-FUT4 cells after cycloheximide (CHX) treatment for the indicated times. (E) ICAM3 expression in KG1a cells treated with CHX in the presence or absence of MG132 or chloroquine (Chlo) for 8 h. (F–J) Immunoblot analysis of NF-κB signaling components (p65, p-p65, IκBα, p-IκBα) and tight junction–related proteins in HUVECs treated with BAY-11-7082 (F, G), phorbol 12-myristate 13-acetate (PMA) (H, I), or sEVs from the indicated cells (J).

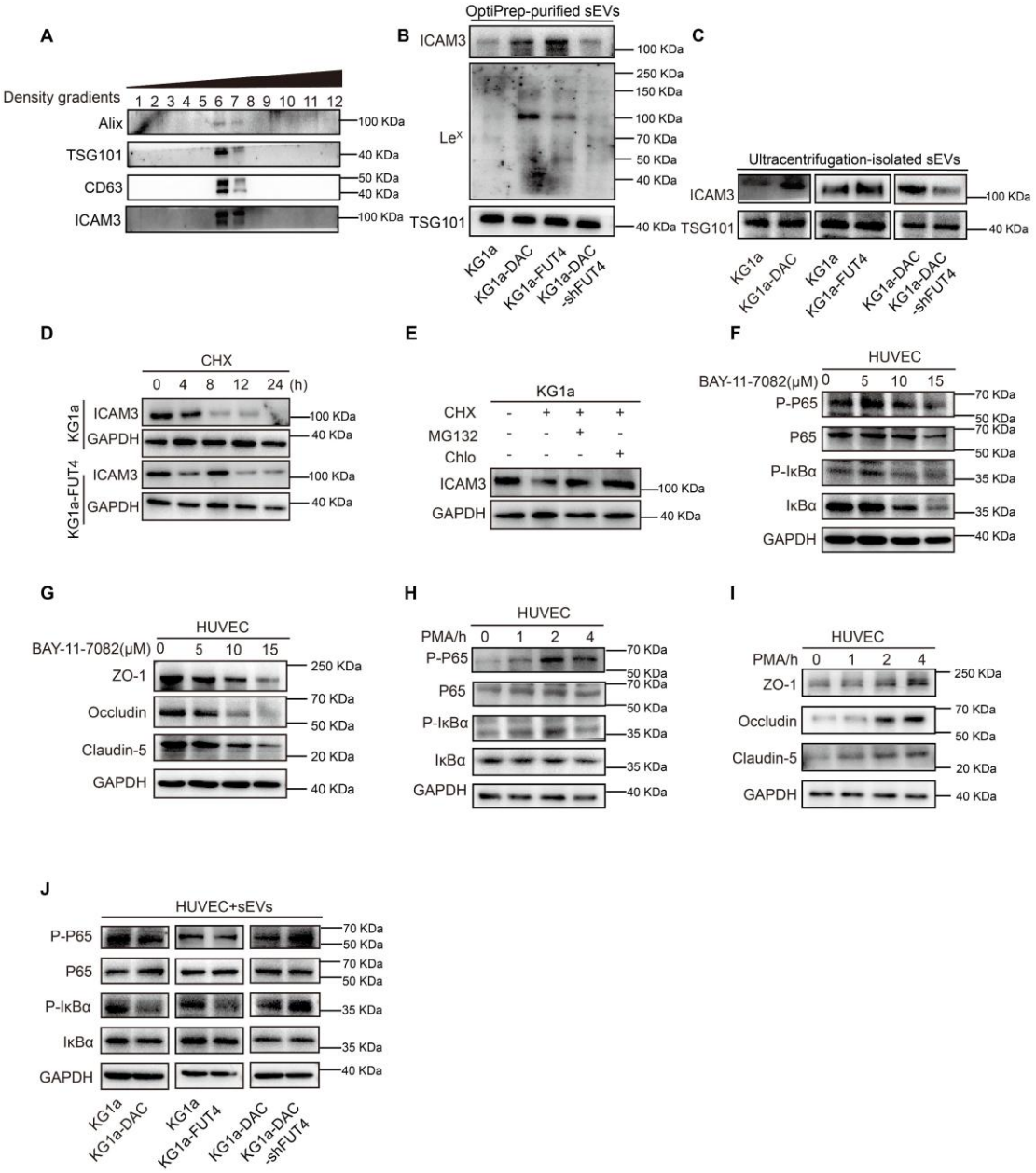

Fig. S8. (A) Expression of tight junction–related proteins and NF-κB signaling components (p65, p-p65, IκBα, p-IκBα) in HUVECs cocultured with KG1a-DAC cells in the presence or absence of anti-human ICAM3 antibody (a-ICAM3). (B, C) HUVEC permeability and leukemic cell transendothelial migration, and (D) angiogenesis metrics of HUVECs cocultured with indicated cells with or without a-ICAM3. (E) Expression of tight junction–related proteins and NF-κB signaling components (p65, p-p65, IκBα, p-IκBα) in HUVECs cocultured with KG1a-DAC-shFUT4 cells with or without

recombinant ICAM3 (rICAM3). (F, G) HUVEC permeability and leukemic cell transendothelial migration, and (H) angiogenesis metrics of HUVECs cocultured with indicated cells with or without rICAM3. (I) Immunoblot analysis of ICAM3 and NF-κB signaling components (p65, p-p65, IκBα, p-IκBα) in HUVEC and HUVEC-ICAM3. (J) Immunoblot analysis of tight junction–related proteins and ICAM3 in HUVEC and HUVEC-ICAM3. (K, L) HUVEC permeability and leukemic cell transendothelial migration in HUVEC and HUVEC-ICAM3. (M) Angiogenesis metrics, including junction count and total branching length, were quantified in HUVEC and HUVEC-ICAM3. Data are mean ± SEM; experiments were repeated three times with similar results. *P<0.05; **P<0.01; ***P<0.001.

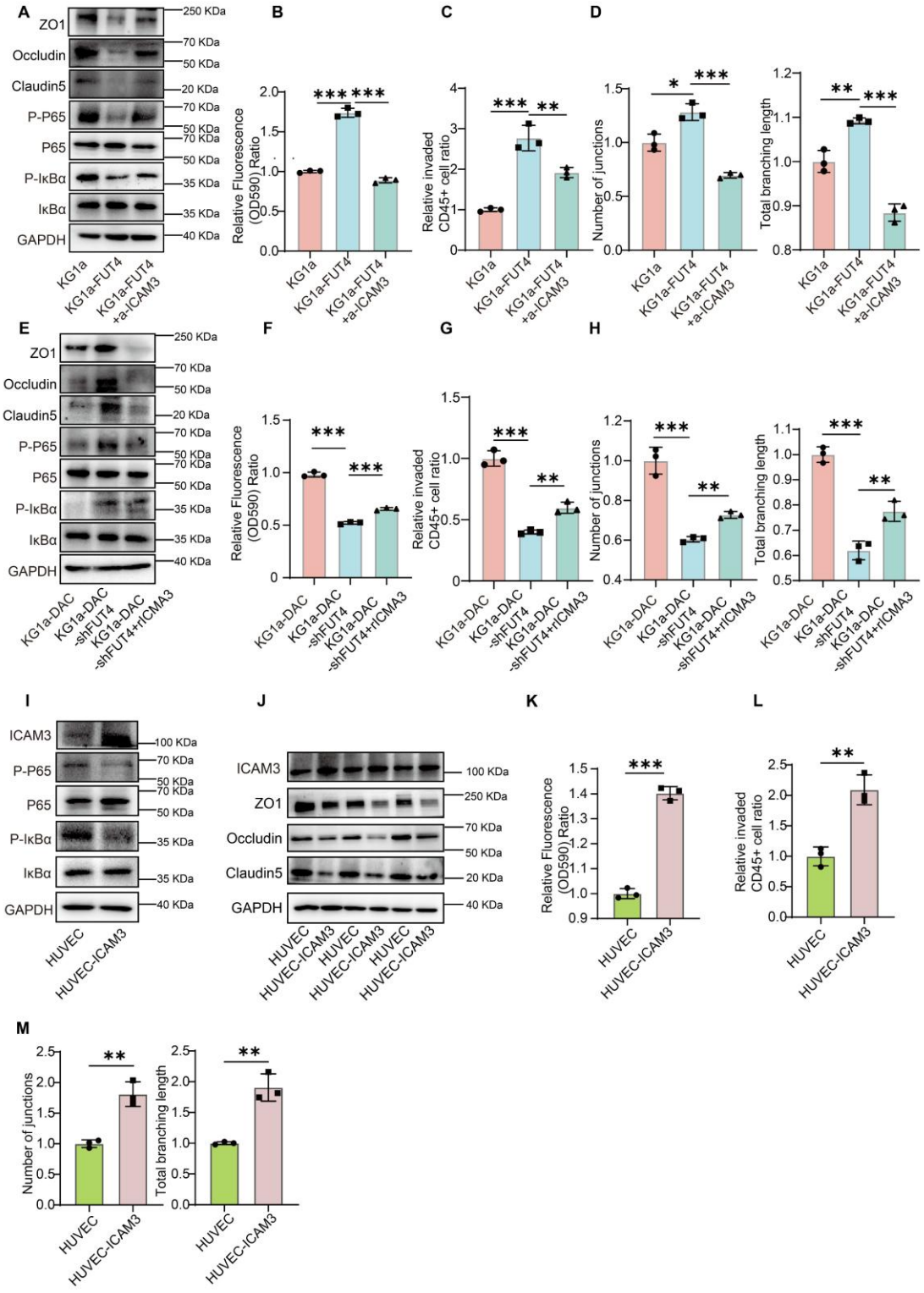

Supplementary tables

Tab. S1 Patients list

Diagnosis	Age	Gender	Cytogenetics	BM Cellularity	Marrow Blast Count	DAC Response

AML	69	M	Normal	Hypercellular	41%	R
MDS-EB2	54	M	Normal	Normal	16.80%	R
AML	73	F	Normal	Hypercellular	43%	R
AML	48	M	Normal	Hypercellular	45%	R
AML	31	F	Normal	Hypercellular	53%	R
AML	48	F	Normal	Hypercellular	61%	R
MDS-EB1	35	M	Normal	Hypercellular	12%	R
MDS-EB2	31	M	Normal	Hypercellular	14%	R
MDS-EB2	56	M	Normal	Hypercellular	13%	R
AML	77	F	Normal	Hypercellular	24%	R
AML	64	M	Normal	Normal	35%	R
MDS-EB2	72	F	Normal	Normal	17%	R
AML	53	F	Normal	Hypercellular	27%	R
AML	62	F	t(8;21)(q22;q22)	Normal	30%	R
MDS-EB2	65	M	Normal	Hypercellular	15%	R
MDS-EB1	75	F	Normal	Hypercellular	12%	R
MDS-EB2	76	F	Normal	Hypercellular	14%	R
AML	67	F	Normal	Hypercellular	25%	R
AML	70	M	Normal	Hypercellular	25%	R
AML	78	F	Normal	Normal	40%	S
MDS-MLD	65	M	Normal	Normal	6.50%	S
MDS-EB1	62	M	Normal	Normal	8%	S
AML	48	M	t(8;21)(q22;q22)	Hypercellular	23.50%	S
AML	58	M	Normal	Hypercellular	29%	S
MDS-EB2	66	F	Complex karyotype	Normal	23%	S
AML	43	F	t(8;21)(q22;q22), +8	Hypercellular	29%	S
AML	58	F	Normal	Normal	32%	S
AML	68	M	Normal	Normal	22%	S
MDS-EB1	44	F	Normal	Normal	5%	S
MDS-EB1	61	F	Normal	Hypercellular	9%	S
MDS-EB2	75	F	Complex karyotype	Hypercellular	14%	S
AML	30	M	Normal	Hypercellular	30%	S
AML	79	M	Normal	Normal	45%	S
AML	32	F	t(8;21)(q22;q22)	Hypercellular	36%	S
AML	68	F	Normal	Hypercellular	28%	S
MDS-EB2	76	M	Complex karyotype	Normal	25%	S

MDS-EB1	74	M	Normal	Normal	8%	S
HD	45	F				
HD	36	F				
HD	35	M				
HD	58	F				
HD	27	M				
HD	36	F				
HD	45	F				
HD	28	F				
HD	61	F				
HD	23	F				
HD	57	M				
HD	60	M				
HD	61	M				
HD	49	M				
HD	28	M				
HD	70	F				
HD	61	F				
HD	69	M				
HD	48	M				

Tab. S2

Identified N-glycans in plasma from HD, DAC-S, and DAC-R patients and in sEVs from KG1a and KG1a-DAC cells, as determined by MALDI-TOF/TOF-MS.

Identified N-glycans in plasma

HD															
	HD1			HD2			HD3			HD4			HD5		
	m/z	Intens.	SN	m/z	Intens.	SN	m/z	Intens.	SN	m/z	Intens.	SN	m/z	Intens.	SN
	1257.442618	48390.37508	7.308849286	1257.442618	62293.86611	8.282067654	1257.442618	62293.86611	8.282067654	1257.442618	76501.40191	9.446165341	1257.442618	85269.98526	9.825447045
	1419.488044	55969.41755	11.36446256	1419.488044	72048.92952	12.73024997	1419.488044	72048.92952	12.73024997	1419.488044	82484.53735	13.05470795	1419.488044	92729.90708	13.61640755
	1485.531899	64886.92396	15.00583201	1485.531899	97183.5025	15.29322584	1485.531899	97183.5025	15.29322584	1485.531899	104951.631	14.86226625	1485.531899	126597.4774	15.70605271
	1540.611308	37323.96203	8.253211112	1540.611308	38424.16326	6.984150025	1540.611308	38424.16326	6.984150025	1540.611308	40052.11765	6.094211535	1540.611308		
	1581.537304			1581.537304			1581.537304			1581.537304			1581.537304	82115.5772	6.335054702
	1647.597034	85107.84379	25.66180191	1647.597034	108610.607	28.5707462	1647.597034	108610.607	28.5707462	1647.597034	124109.1022	28.67411277	1647.597034	137298.2033	29.59432139
	1688	34089.98876	9.44281318	1688	36175.09889	8.360627515	1688			1688	38157.73889	7.321229131	1688		
	1743.583768	39695.70528	11.91248086	1743.583768	46630.12139	12.16573529	1743.583768	46630.12139	12.16573529	1743.583768	53256.36801	12.00056758	1743.583768	58628.44915	12.30692476
	1809.645023	46869.10792	15.94665852	1809.645023	62220.26468	18.86445687	1809.645023	62220.26468	18.86445687	1809.645023	71345.40772	18.79753637	1809.645023	75783.84707	18.51682198
	1850.683064			1850.683064			1850.683064			1850.683064	28164.64319	6.11931064	1850.683064	30571.07964	6.066477547
	1905.621898	36173.81323	13.73536551	1905.621898	43467.43828	14.41116422	1905.621898	43467.43828	14.41116422	1905.621898	46012.71334	12.85872113	1905.621898	49168.86137	12.58302223
	1976.66371	27140.32741	10.93299734	1976.66371	40280.88042	14.76066018	1976.66371	40280.88042	14.76066018	1976.66371	45598.77318	14.15679913	1976.66371	49852.88305	14.36935699
	2122.696568			2122.696568	18606.33754	7.041762149	2122.696568	18606.33754	7.041762149	2122.696568	23039.28514	7.416200639	2122.696568	26046.28301	7.827581162
	2289.673503	29517.68258	19.42465148	2289.673503	39516.85726	22.97095839	2289.673503	39516.85726	22.97095839	2289.673503	51695.14417	25.86174345	2289.673503	56117.68601	26.0141804
Relative Intensity															
	1257.442618	0.095791199		1257.442618	0.093610506		1257.442618	0.09899182		1257.442618	0.097408244		1257.442618	0.097991176	
	1419.488044	0.110794297		1419.488044	0.108269676		1419.488044	0.114493691		1419.488044	0.105026493		1419.488044	0.106564023	
	1485.531899	0.128446953		1485.531899	0.14604001		1485.531899	0.154435298		1485.531899	0.133633552		1485.531899	0.145484202	
	1540.611308	0.073884674		1540.611308	0.057740923		1540.611308	0.061060231		1540.611308	0.050997843		1540.611308	0	
	1581.537304	0		1581.537304	0		1581.537304	0		1581.537304	0		1581.537304	0.094366171	
	1647.597034	0.168475288		1647.597034	0.163211797		1647.597034	0.172594226		1647.597034	0.158026512		1647.597034	0.157781339	
	1688	0.06748286		1688	0.0543612		1688	0		1688	0.048585755		1688	0	
	1743.583768	0.078579659		1743.583768	0.070072216		1743.583768	0.074100403		1743.583768	0.067810643		1743.583768	0.067375064	
	1809.645023	0.092779773		1809.645023	0.093499903		1809.645023	0.098874859		1809.645023	0.090843183		1809.645023	0.087089828	
	1850.683064	0		1850.683064	0		1850.683064	0		1850.683064	0.035861675		1850.683064	0.035131894	
	1905.621898	0.071607896		1905.621898	0.065319575		1905.621898	0.069074551		1905.621898	0.058587392		1905.621898	0.056504227	
	1976.66371	0.053725653		1976.66371	0.060531057		1976.66371	0.064010759		1976.66371	0.058060327		1976.66371	0.057290295	
	2122.696568	0		2122.696568	0.027960195		2122.696568	0.029567521		2122.696568	0.029335623		2122.696568	0.029932055	
	2289.673503	0.058431748		2289.673503	0.059382941		2289.673503	0.062796642		2289.673503	0.065822757		2289.673503	0.064489727	
DAC-S															
	DAC-S1			DAC-S2			DAC-S3			DAC-S4			DAC-S5		
	m/z	Intens.	SN	m/z	Intens.	SN	m/z	time	SN	m/z	Intens.	SN	m/z	Intens.	SN
	1257.442618	33745.85484	6.787765372	1257.442618	38468.37508	7.308849286	1257.427555	15725.36285	14.81545153	1257.442618	13213.00242	13.54818022	1257.442618	38468.37508	7.308849286
	1419.488044	42165.0417	10.76846517	1419.488044	46949.66755	11.36446256	1419.483485	19463.79779	20.31663866	1419.488044	14686.5498	16.90778107	1419.488044	46949.66755	11.36446256
	1485.531899	46817.11293	13.12261146	1485.531899	56290.42396	15.00583201	1485.549465	82909.15767	58.49198609	1485.531899	88260.29547	71.74218796	1485.531899	56290.42396	15.00583201
	1540.611308	29423.54933	8.942215411	1540.611308	28709.96203	8.253211112	1540.611308			1540.611308			1540.611308	28709.96203	8.253211112
	1581.537304			1581.537304			1581.537304			1581.537304			1581.537304		
	1647.597034	69064.21393	24.11389804	1647.597034	77991.34379	25.66180191	1647.609478	39993.71442	48.16391546	1647.597034	33126.09221	44.93303167	1647.597034	77991.34379	25.66180191
	1688			1688			1688.635944			1688.635944	7400.889123	9.741297745	1688		
	1743.583768	30050.16193	11.79804178	1743.583768	32835.20528	11.91248086	1743.612004	6573.231778	7.795538042	1743.583768			1743.583768	32835.20528	11.91248086
	1809.645023	36989.82259	15.61897235	1809.645023	40857.60792	15.94665852	1809.66241	8810.673648	11.2187341	1809.645023	8257.320121	12.01976704	1809.645023	40857.60792	15.94665852
	1850.683064			1850.683064			1850.684132	5973.437826	7.604367703	1850.683064	6204.440411	9.102925528	1850.683064		
	1905.621898	28211.59926	13.83008261	1905.621898	30446.31323	13.73536551	1905.621898			1905.621898	5366.346492	9.121018217	1905.621898	30446.31323	13.73536551
	1976.66371	17654.16837	9.630258983	1976.66371	21859.82741	10.93299734	1976.669542	11357.8789	17.25591935	1976.66371			1976.66371	21859.82741	10.93299734
	2122.696568			2122.696568			2122.690384	5189.26062	8.872784195	2122.696568			2122.696568		
	2289.673503	21650.07167	17.79588306	2289.673503	25752.18258	19.42465148	2289.669339	28853.63872	62.75449252	2289.673503	5885.797504	14.29788471	2289.673503	25752.18258	19.42465148
Relative Intensity															
	1257.442618	0.094852583		1257.442618	0.096132266		1257.442618	0.069937078		1257.442618	0.072439415		1257.442618	0.096132266	
	1419.488044	0.118517167		1419.488044	0.117326972		1419.488044	0.086563418		1419.488044	0.080518041		1419.488044	0.117326972	
	1485.531899	0.131593172		1485.531899	0.140669473		1485.531899	0.368730713		1485.531899	0.483881253		1485.531899	0.140669473	
	1540.611308	0.082703481		1540.611308	0.071746044		1540.611308	0		1540.611308	0		1540.611308	0.071746044	
	1581.537304	0		1581.537304	0		1581.537304	0		1581.537304	0		1581.537304	0	
	1647.597034	0.194125148		1647.597034	0.194899957		1647.597034	0.177868299		1647.597034	0.181611617		1647.597034	0.194899957	
	1688	0		1688	0		1688	0		1688	0.040574887		1688	0	
	1743.583768	0.084464758		1743.583768	0.082055005		1743.583768	0.029233833		1743.583768	0		1743.583768	0.082055005	
	1809.645023	0.103970702		1809.645023	0.102102947		1809.645023	0.039184646		1809.645023	0.045270213		1809.645023	0.102102947	
	1850.683064	0		1850.683064	0		1850.683064	0.026566305		1850.683064	0.034015436		1850.683064	0	
	1905.621898	0.079296941		1905.621898	0.076085176		1905.621898	0		1905.621898	0.029420641		1905.621898	0.076085176	
	1976.66371	0.049622197		1976.66371	0.054627593		1976.66371	0.050513103		1976.66371	0		1976.66371	0.054627593	
	2122.696568	0		2122.696568	0		2122.696568	0.023078751		2122.696568	0		2122.696568	0	
	2289.673503	0.060853851		2289.673503	0.064354568		2289.673503	0.128323856		2289.673503	0.032268497		2289.673503	0.064354568	
DAC-R															

Identified N-glycans in plasma

	DAC-R1			DAC-R2			DAC-R3			DAC-R4			DAC-R5		
	m/z	Intens.	SN	m/z	Intens.		m/z	Intens.	SN	m/z	Intens.	SN	m/z	Intens.	SN
	1257.442618	10591.41845	10.88109187	1257.442618			1257.442618	10918.4106	10.2125309	1257.442618	11239.21486	11.04326109	1257.442618	17748.25	6.760248562
	1419.488044	11940.65614	13.38365305	1419.488044	56415.50221	33.41839438	1419.488044	11419.39229	11.95547211	1419.488044	12071.59178	13.62242043	1419.488044		
	1485.531899	96472.26061	117.2583825	1485.531899			1485.531899	55594.45518	133.2316425	1485.531899	48556.72181	84.75072329	1485.531899	25016.60922	
	1540.611308			1540.611308			1540.611308			1540.611308			1540.611308		
	1581.537304			1581.537304			1581.537304			1581.537304			1581.537304	8676.375	6.304286005
	1647.597034	65512.12298	87.68486452	1647.597034	24789.00571	17.60448954	1647.597034	80970.47459	104.8850487	1647.597034	43165.40819	60.73208538	1647.597034	45016.60922	10.2176271
	1688.635944	5132.963819	6.455563105	1688.635944			1688	6044.786872	7.425399895	1688			1688.635944	7752.25	5.89281378
	1743.583768	5132.963819	6.455563105	1743.583768			1743.583768			1743.583768			1743.583768	9494.90625	6.133134899
	1809.645023	12640.23528	18.39792797	1809.645023	3150.75	6.404533639	1809.645023	20580.42119	29.58831737	1809.645023	8016.535647	12.29296593	1809.645023		
	1850.683064	5536.786699	7.929526088	1850.683064			1850.683064	7455.886833	10.54131245	1850.683064			1850.683064		
	1905.621898			1905.621898			1905.621898			1905.621898			1905.621898	9841.5	7.039311893
	1976.66371	5163.49141	8.573837825	1976.66371	5328	7.927429414	1976.66371	9491.006684	15.98274193	1976.66371	5029.257511	9.135098363	1976.66371		
	2122.696568			2122.696568			2122.696568	3400.629462	6.384596458	2122.696568			2122.696568		
	2289.673503	3940.219176	9.265716749	2289.673503			2289.673503	6471.837977	15.38398936	2289.673503	2812.980308	7.232656147	2289.673503		
Relative Intensity															
	1257.442618	0.047695531		1257.442618	0		1257.442618	0.051417704		1257.442618	0.085866514		1257.442618	0.143656437	
	1419.488044	0.053771451		1419.488044	0.583488503		1419.488044	0.05377696		1419.488044	0.092225793		1419.488044	0	
	1485.531899	0.434436215		1485.531899	0		1485.531899	0.261809096		1485.531899	0.370968656		1485.531899	0.202487398	
	1540.611308	0		1540.611308	0		1540.611308	0		1540.611308	0		1540.611308	0	
	1581.537304	0		1581.537304	0.022141131		1581.537304	0		1581.537304	0		1581.537304	0.070227607	
	1647.597034	0.295015775		1647.597034	0.2563852		1647.597034	0.38131153		1647.597034	0.329779542		1647.597034	0.364369766	
	1688	0.023114887		1688	0		1688	0.028466511		1688	0		1688	0.06274763	
	1743.583768	0.023114887		1743.583768	0		1743.583768	0		1743.583768	0		1743.583768	0.076852896	
	1809.645023	0.056921813		1809.645023	0.032587256		1809.645023	0.096918685		1809.645023	0.061245557		1809.645023	0	
	1850.683064	0.024933392		1850.683064	0		1850.683064	0.035111757		1850.683064	0		1850.683064	0	
	1905.621898	0		1905.621898	0		1905.621898	0		1905.621898	0		1905.621898	0.079658267	
	1976.66371	0.023252359		1976.66371	0.055105895		1976.66371	0.044695678		1976.66371	0.038423041		1976.66371	0	
	2122.696568	0		2122.696568	0		2122.696568	0.01601447		2122.696568	0		2122.696568	0	
	2289.673503	0.01774369		2289.673503	0		2289.673503	0.030477609		2289.673503	0.021490897		2289.673503	0	

Stastic analysis for plasma

			Relative intensity															Average intensity			Fold change	
Component		Calculated.mass	HD1	HD2	HD3	HD4	HD5	DAC-S-1	DAC-S-2	DAC-S-3	DAC-S-4	DAC-S-5	DAC-R-1	DAC-R-2	DAC-R-3	DAC-R-4	DAC-R-5	HD	DAC-S	DAC-R	DAC-S/HD	DAC-R/HD
HexNAc(2)Hex(5)	N2H5	1257.423	0.090	0.094	0.099	0.097	0.098	0.095	0.096	0.070	0.072	0.096	0.048	0.000	0.051	0.086	0.144	0.095	0.080	0.066	0.836	0.691
HexNAc(2)Hex(6)	N2H6	1419.476	0.105	0.108	0.114	0.105	0.107	0.111	0.112	0.087	0.081	0.117	0.119	0.340	0.054	0.092	0.059	0.108	0.104	0.133	0.964	1.227
HexNAc(2)Hex(7)	N2H7	1581.528	0.000	0.000	0.000	0.000	0.101	0.000	0.000	0.000	0.000	0.000	0.000	0.013	0.000	0.000	0.070	0.000	0.000	0.017	/	/
HexNAc(2)Hex(8)	N2H8	1743.584	0.074	0.070	0.074	0.068	0.067	0.084	0.082	0.029	0.000	0.082	0.023	0.000	0.000	0.000	0.077	0.072	0.050	0.020	0.701	0.279
HexNAc(2)Hex(9)	N2H9	1905.634	0.068	0.065	0.069	0.059	0.057	0.079	0.076	0.000	0.029	0.076	0.000	0.000	0.000	0.000	0.080	0.065	0.043	0.016	0.667	0.245
HexNAc(4)Hex(3)Fuc(1)	N4H3F1	1485.534	0.177	0.146	0.154	0.134	0.145	0.132	0.141	0.369	0.484	0.141	0.434	0.149	0.262	0.371	0.202	0.153	0.283	0.356	1.854	2.327
HexNAc(4)Hex(4)Fuc(1)	N4H4F1	1647.587	0.159	0.163	0.173	0.158	0.158	0.194	0.195	0.178	0.182	0.195	0.295	0.270	0.381	0.330	0.364	0.163	0.206	0.328	1.265	2.010
HexNAc(4)Hex(5)NeuAc(1)	N4H5S1	1976.730	0.051	0.061	0.064	0.058	0.057	0.084	0.082	0.051	0.000	0.082	0.023	0.032	0.045	0.000	0.121	0.058	0.054	0.044	0.921	0.757
HexNAc(4)Hex(5)Fuc(1)	N4H5F1	1809.639	0.088	0.093	0.099	0.091	0.087	0.104	0.102	0.039	0.045	0.102	0.057	0.033	0.097	0.061	0.000	0.093	0.075	0.050	0.808	0.534
HexNAc(4)Hex(5)Fuc(1)NeuAc(1)	N4H5F1S1	2122.735	0.000	0.028	0.030	0.029	0.030	0.000	0.000	0.023	0.000	0.000	0.000	0.000	0.012	0.000	0.000	0.022	0.004	0.002	0.177	0.115
HexNAc(4)Hex(5)Fuc(2)NeuAc(1)	N5H4F2S1	2289.674	0.055	0.059	0.063	0.066	0.064	0.061	0.064	0.128	0.032	0.064	0.018	0.015	0.024	0.038	0.000	0.061	0.061	0.019	1.009	0.313
HexNAc(5)Hex(3)	N5H3	1542.555	0.070	0.058	0.061	0.051	0.000	0.083	0.072	0.000	0.000	0.072	0.000	0.000	0.000	0.000	0.000	0.060	0.038	0.000	0.630	0.000
HexNAc(5)Hex(3)Fuc(1)	N5H3F1	1688.613	0.064	0.054	0.000	0.049	0.000	0.000	0.000	0.000	0.049	0.000	0.023	0.024	0.016	0.000	0.063	0.042	0.012	0.025	0.287	0.606
HexNAc(5)Hex(4)Fuc(1)	N5H4F1	1850.666	0.000	0.000	0.000	0.036	0.035	0.000	0.000	0.027	0.034	0.000	0.025	0.000	0.030	0.021	0.000	0.009	0.014	0.015	1.590	1.716

Identified N-glycans in sEVs

K1				K2				K3			
	m/z	Intens.	SN		m/z	Intens.	SN		m/z	Intens.	SN
	1256.5408	18085.1012	65.6570		1256.5258	10642.8881	93.5570		1257.4336	2463.6092	18.8929
	1418.6021	7381.7889	27.6157		1418.5749	4323.2574	40.2809		1419.4753	1398.2454	11.3651
									1975.8219	686.8860	7.1666
KD-1				KD-2				KD-3			
	m/z	Intens.	SN		m/z	Intens.	SN		m/z	Intens.	SN
	1257.5570	45075.7553	257.6766		1257.5086	43058.4785	275.6597		1257.5204	39894.0745	279.4315
	1419.6096	21806.0062	132.4888		1419.5600	24333.7562	164.5564		1419.5743	24691.2988	186.6351
	1485.6997	1560.3371	9.8465		1485.6177	1594.8664	11.1529		1485.6434	1556.6989	12.0008
	1581.6815	1270.2628	8.3226		1581.6105	890.9371	6.4359		1581.6150	980.1237	7.7876
	1647.7975	1455.7467	10.6072		1647.6807	1490.9277	11.0752		1647.6973	1272.1185	10.3708
	1743.7169	2491.3209	18.1089		1743.6586	1296.7750	10.0187		1743.6811	1152.8104	9.7135
	1809.8583	1113.8663	8.5417						1976.8031	805.7485	8.4492
	1976.1179	914.5810	9.1344								
	2012.9892	587.7318	6.0635								

Stastic analysis for sEVs

			Relative intensity						Average intensity	
		Calculated.mass	KG1a-sEVs-1	KG1a-sEVs-2	KG1a-sEVs-3	KG1a-DAC-sEVs-1	KG1a-DAC-sEVs-2	KG1a-DAC-sEVs-3	KG1a-sEVs	KG1a-DAC-sEVs
HexNAc(2)Hex(5)	N2H5	1257.557	0.710	0.711	0.542	0.591	0.593	0.567	0.654	0.615
HexNAc(2)Hex(6)	N2H6	1419.610	0.290	0.289	0.307	0.286	0.335	0.351	0.295	0.294
HexNAc(2)Hex(7)	N2H7	1581.682	0.000	0.000	0.000	0.017	0.012	0.014	0.000	0.006
HexNAc(2)Hex(8)	N2H8	1743.584	0.000	0.000	0.000	0.033	0.018	0.016	0.000	0.011
HexNAc(4)Hex(3)Fuc(1)	N4H3F1	1485.700	0.000	0.000	0.000	0.020	0.022	0.022	0.000	0.007
HexNAc(4)Hex(4)Fuc(1)	N4H4F1	1647.797	0.000	0.000	0.000	0.019	0.021	0.018	0.000	0.006
HexNAc(4)Hex(5)Fuc(1)	N4H5F1	1809.858	0.000	0.000	0.000	0.015	0.000	0.000	0.000	0.005
HexNAc(4)Hex(5)NeuAc(1)	N4H5S1	1976.118	0.000	0.000	0.151	0.012	0.000	0.011	0.050	0.054
HexNAc(5)Hex(5)Fuc(1)	N5H5F1	2012.989	0.000	0.000	0.000	0.008	0.000	0.000	0.000	0.003

Tab. S3 Primer list for chip

Primers	Sequences
FUT4-E-box-1-F	CGAGGTAAGAGGGCACAAAGAAAAT
FUT4-E-box-1-R	AGGCATTTGGGAAATATTACCCTGC
FUT4-E-box-2-F	GCCACGTGCCAGACACAATGTT
FUT4-E-box-2-R	AGGTGTTCTGGCTAGGCCCAT
FUT4-E-box-3-F	TCTCGATCTCCTGACCT
FUT4-E-box-3-R	ATTTGCGTTAGCCATATG
FUT4-E-box-4-F	AACACCTGGCAGGATTG
FUT4-E-box-4-R	AGCTGTGCATCAGTGGA
FUT4-E-box-5-F	AGTATCAGTGGGACTCCACT
FUT4-E-box-5-R	TCTGGGTGTTCGCTTTG
FUT4-E-box-6-F	TCTCAAGTGACTGTAGACGT
FUT4-E-box-6-R	ATTCTAGCACCCAAGTTAAGG
FUT4-E-box-7-F	GTTCTCTATCCTTTACTGGGCT
FUT4-E-box-7-R	AGACGGTCGAATTGTGGAG

Tab. S4 Primer list for dual luciferase reporter assay

Primers	Sequences
FUT4-F	AGATCGCCGTGTAATTCTAGATGCGAAGTCACGACTGGTTTC
FUT4-R	AGGGCATCGGTCGACGGATCCGGAGGATAGCGTCGGCTTCC
FUT4-E-BOX-1F'	GTAATATTTCCACAATGCCTACCGGCCACGT
FUT4-E-BOX-1R'	CGGTAGGCATTGTGGAAATATTACCCTGCTTGATTGC

FUT4-E-BOX-2F'	TACCGGCACCGTGCCAGACACAAT
FUT4-E-BOX-2R'	ATTGTGTCTGGCACGGTGCCGGTAGGCATTTGGGA
FUT4-E-BOX-7F'	CACACAATGCAGAGACTCTGAAGGCCA
FUT4-E-BOX-7R'	CCTTCAGAGTCTCTGCATTGTGTGAAGAACTTAAG

Supplemental Reference

1. Lei L, Wang Y, Liu R, et al. Transfer of miR-4755-5p through extracellular vesicles and particles induces decitabine resistance in recipient cells by targeting CDKN2B. Mol Carcinog. 2023;62(6):743-753.

2. Sung BH, Ketova T, Hoshino D, Zijlstra A, Weaver AM. Directional cell movement through tissues is controlled by exosome secretion. Nat Commun. 2015;6:7164.

3. Beer LA, Liu P, Ky B, Barnhart KT, Speicher DW. Efficient Quantitative Comparisons of Plasma Proteomes Using Label-Free Analysis with MaxQuant. Methods Mol Biol. 2017;1619:339-352.

4. Cao L, Zhou Y, Li X, Lin S, Tan Z, Guan F. Integrating transcriptomics, proteomics, glycomics and glycoproteomics to characterize paclitaxel resistance in breast cancer cells. J Proteomics. 2021;243:104266.

5. Ceroni A, Maass K, Geyer H, Geyer R, Dell A, Haslam SM. GlycoWorkbench: a tool for the computer-assisted annotation of mass spectra of glycans. J Proteome Res. 2008;7(4):1650-1659.

6. Wang R, Liu Y, Wang C, et al. Comparison of the methods for profiling N-glycans-hepatocellular carcinoma serum glycomics study. RSC Adv. 2018;8(46):26116-26123.

7. Ramachandran P, Xu G, Huang HH, et al. Serum Glycoprotein Markers in Nonalcoholic Steatohepatitis and Hepatocellular Carcinoma. J Proteome Res. 2022;21(4):1083-1094.

8. Tsai TH, Wang M, Di Poto C, et al. LC-MS profiling of N-Glycans derived from human serum samples for biomarker discovery in hepatocellular carcinoma. J Proteome Res. 2014;13(11):4859-4868.

9. Li H, Wang Y, Feng S, et al. Reciprocal regulation of TWIST1 and OGT determines the decitabine efficacy in MDS/AML. Cell Commun Signal. 2023;21(1):255.

10. Li H, Wang Y, Pang X, et al. Elevated TWIST1 expression in myelodysplastic syndromes/acute myeloid leukemia reduces efficacy of hypomethylating therapy with decitabine. Haematologica. 2020;105(10):e502.

11. Tan Z, Cao L, Wu Y, et al. Bisecting GlcNAc modification diminishes the pro-metastatic functions of small extracellular vesicles from breast cancer cells. J Extracell Vesicles. 2020;10(1):e12005.